ISSN 0973-2063 (online) 0973-8894 (print)

Bioinformation 22(7): 3954-3962 (2026)

BIOINFORMATION
Discovery at the interface of physical and biological sciences

BIOMEDICAL INFORMATICS

www.bioinformation.net

Volume 22(7)

Research Article

Received July 1, 2026; Revised July 31, 2026; Accepted July 31, 2026, Published July 31, 2026

DOI: 10.6026/973206300223954

SJIF 2026 (Scientific Journal Impact Factor for 2026) = 8.478
2022 Impact Factor (2023 Clarivate Inc. release) is 1.9

Edited by P Kangueane
Citation: Wu Bioinformation 22(7): 3954-3962 (2026)

SPADE: An R package for spatial proximity analysis of differential expression

Mingke Wu*

Department of Immunology, School of Basic Medical Sciences, Peking University, Beijing, 100191, China; *Corresponding author

Affiliation URL:
https://www.pku.edu.cn/

Author contact:
Mingke Wu - E-mail: mingkewu@stu.pku.edu.cn

Abstract:
Spatial transcriptomics enables characterization of tissue organization *in situ*, but accurate identification of spatially resolved transcriptional changes remains challenging because spot-level measurements are confounded by mixed-cell signals and

ISSN 0973-2063 (online) 0973-8894 (print)
Bioinformation 22(7): 3954-3962 (2026)

contamination from neighboring cells. We developed SPADE, an R package integrated with Seurat, to identify contamination-aware differential expression between cells located near versus far from a reference cell type. Applying SPADE to 25 human NSCLC samples and validating findings in an independent cohort, we identified conserved distance-dependent transcriptional programs in tumor-proximal endothelial, stromal and immune cells, including pathways related to vascular homeostasis, extracellular matrix remodeling, antigen presentation and inflammatory signaling. Thus, data shows the spatially coordinated tumor microenvironment remodeling and demonstrate that accounting for spatial contamination improves the robustness of spatial transcriptomic inference. SPADE enables systematic discovery of spatial transcriptional reprogramming in complex tissues.

Keywords: Spatial transcriptomics, differential expression analysis, R package, cell-cell interaction, non-small cell lung cancer (NSCLC)

Background:

Spatial transcriptomics has revolutionized biomedical research by integrating gene expression with spatial localization and enabling the decoding of cellular communication **[1, 2]**. However, a critical analytical gap remains: Most existing computational tools lack the capacity to quantify how gene expression changes in various distances **[3, 4]**. For example, understanding how stromal cells transcriptionally adapt at 50 µm versus 200 µm from a tumor boundary is fundamental to studying metastatic niches **[5]**. The challenge is further compounded by the inherent technical limitations of Spatial technologies **[6]**. Unlike single-cell resolution, most spatial spots capture 5 to 20 cells per capture area. In addition, most existing annotation methods will regard each spot as a mixture of multiple cell types, even when one cell type constitutes most of the spot **[7, 8]**. This leads to pervasive gene expression contamination, where signals from adjacent cells influence the expression of an ideal cell type **[9]**. Consequently, when attempting to compare spatially resolved differential expression, the true biological shifts in response to distance cannot be reliably discovered **[10, 11]**. Therefore, it is of interest to report that SPADE enables contamination-aware spatial differential expression analysis and reveals reproducible spatial reprogramming across multiple cell types in the NSCLC tumor microenvironment.

Methods:

Cell selection and distance calculation:

For each pair of target cell types (cell A vs cell B), SPADE identifies cells of each type based on metadata annotations. Euclidean distances from each cell A to the nearest cell B are computed using the get.knnx function from the FNN package.

Grouping by spatial proximity:

Cell A are first classified into near, mid and far groups based on user-defined distance thresholds relative to Cell B. Differential expressed genes between the near and far groups will be initially identified using Seurat's Find Markers function (log fold-change threshold = 0.25, minimum detection fraction = 10%). To remove potential confounding effects from neighboring Cell B, SPADE selects the closest Cell B for each Cell A as a control cluster. Genes that are differentially expressed between this control cluster and the far group of Cell A are then excluded from the initial near-vs-far list, effectively filtering signals that may result from contamination from Cell B genes. This two-step filtering ensures that the final list of differential genes reflects true spatially

Associated differences:

Functional enrichment analysis:

Significantly upregulated and downregulated genes (adjusted p-value < 0.05) are mapped from gene symbols to Entrez IDs using clusterProfiler::bitr. And Gene Ontology (GO) biological process enrichment is performed with clusterProfiler::enrichGO. Gene set enrichment analysis (GSEA) is performed on the ranked gene list using clusterProfiler::gseGO.

Visualization:

Spatial distribution of distances and groups (near, mid and far) are visualized using SpatialFeaturePlot and SpatialDimPlot in Seurat. Color gradients indicate distance from the reference cell type and distinct colors highlight spatial proximity groups.

Implementation and usage:

SPADE is implemented in R (version ≥ 4.2) and depends on Seurat, FNN, clusterProfiler and org.Hs.eg.db. The package provides a single wrapper function, run_spade_full that automates distance calculation, differential expression, functional enrichment and spatial visualization. SPADE is open-source and available at https://github.com/sorrymaker03/SPADE. SPADE can be installed directly from GitHub using the devtools package: devtools::install_github ("sorrymaker03/SPADE"). The main function run_spade_full requires a spatial transcriptomics object (*e.g.,* Seurat object with spatial coordinates), along with user-defined cell type groups and distance thresholds. In this workflow, SPADE automatically computes distances between specified cell populations, classifies cells into spatial proximity groups, performs differential expression analysis, applies control-based filtering and outputs both table results and spatial visualizations to the user-designated directory.

Data and code availability:

All SPADE source code and usage documentation are available at https://github.com/sorrymaker03/SPADE. The package can be installed via devtools::install_github ("sorrymaker03/SPADE"). A demo spatial transcriptomics dataset derived from a human lung neuroendocrine carcinoma sample, provided by 10x Genomics (https://www.10xgenomics.com/datasets/human-lung-cancer-

11-mm-capture-area-ffpe-2-standard), is included to illustrate package functionality. All spatial transcriptomics data used in this study are publicly available and no new human or animal experiments were conducted. The discovery cohort samples were obtained from GSE307534. The validation cohort samples were obtained from spatial transcriptomics (10x Visium) of human non-small cell lung cancer (NSCLC) **[12]**.

Results:

SPADE: An R package for contamination-aware Spatial Proximity Analysis of Differential Expression We developed SPADE to identify differentially expressed genes between cells proximal versus distal to a reference cell type. SPADE integrates with Seurat objects, using spatial coordinates and cell-type annotations. It calculates the distance from each cell to its nearest reference cell, then compares expression between cells within a "near" versus "far" distance threshold, with a separate control analysis for confounding expression changes (**Figure 1A**). We briefly demonstrate SPADE on a human lung cancer spatial transcriptomics sample. To explore the impact of spatially adjacent myeloid cells on tumor cells, we utilized SPADE to analyze epi-like lung tumor cells located proximal and distal to myeloid cells. The gene expression in nearby spatial clusters would significantly contaminate their adjacent cells, as epi-like tumor cells near myeloid cells have a high expression of LYZ and IFIT3, which is the marker gene of myeloid cells (**Figure 1B-D**). Downstream analyses further found that tumor cells located close to myeloid cells initiated a strong antiviral immune program. Except for two related genes IFI16 and LGALS3BP were significantly upregulated, enrichment analysis clearly showed that the entire interferon response pathway (type I interferon signaling and response to virus) was systematically activated in proximal tumor cells (**Figure 1E**). Simultaneously, pathways related to antigen processing and presentation were also significantly enriched (**Figure 1F**). This characteristic suggests that tumor cells mimic a viral infection state near myeloid cells, which may enhance their antigen presentation ability and thus be more effectively recognized by the immune system. To systematically evaluate SPADE, we applied it to 25 NSCLC spatial transcriptomics samples (283,052 spots) with 10 pre-annotated cell types (**Figure 2A-C**). For each sample, we identified DEGs between TME cells near versus far from tumor cells. We then compiled these DEGs into gene sets and validated them in an independent cohort of 20 samples (**Figure 2A**), testing whether the spatial expression patterns were reproducible. Spatially Proximal Endothelial Cells Exhibit Vascular Homeostasis and Immune-Responsive Programs in NSCLC We used SPADE to compare endothelial cells proximal versus distal to malignant cells across 25 NSCLC samples, retaining genes significant in at least three samples (**Figure 3A**). Tumor-proximal endothelial cells demonstrated upregulation of several genes with established relevance to lung vascular biology and tumor-associated endothelial regulation **[13]**. For example, TMEM100 and EPAS1 are associated with pulmonary endothelial specialization and hypoxia-responsive vascular remodeling **[14, 15]**, while AQP1 and HPGD are implicated in endothelial barrier integrity and anti-inflammatory regulation **[16]**. COL15A1 and PI16 have also been reported in specialized vascular niches and stromal-associated endothelial remodeling **[17]**. Collectively, these findings suggest that endothelial cells adjacent to tumor cells may retain or adapt lung-specific vascular programs while simultaneously responding to the evolving tumor microenvironment. In contrast, endothelial cells located farther from tumor cells exhibited enrichment of genes including SULF1, TIMP1, SFRP4, PLAU, THBS2 and CXCL8, which are implicated in extracellular matrix remodeling, inflammatory signaling, endothelial-to-mesenchymal transition and pro-tumorigenic vascular remodeling **[18]**. These patterns are consistent with prior reports describing activated tumor endothelial phenotypes characterized by fibrosis-like remodeling, aberrant angiogenesis and inflammatory micro environmental interactions. To validate the biological consistency of the tumor-proximal endothelial signature, we applied module scoring of the identified upregulated gene set in another independent NSCLC spatial transcriptomic cohort (**Figure 3B**). Importantly, endothelial cells spatially adjacent to tumor regions similarly exhibited elevated scores for the proximal endothelial program, demonstrating that the identified signature is reproducible across datasets. Gene Set Enrichment Analysis of tumor-proximal endothelial upregulated genes revealed significant enrichment in pathways related to response to stimulus, cellular stress responses, signal transduction and immune activation (**Figure 3C**). Particularly notable was the enrichment of B cell receptor signaling, adaptive immune response, lymphocyte-mediated immunity and immune response-regulating signaling pathways. These results suggest that endothelial cells near tumor cells are not merely passive vascular structures but may actively participate in immune modulation within the NSCLC microenvironment. Tumor-Proximal Stromal Cells Display Activated ECM Remodeling and Immunomodulatory Programs in addition to endothelial cells, stromal fibroblast populations also exhibited pronounced spatial transcriptional remodeling in response to tumor proximity. Tumor-proximal stromal cells exhibited upregulation of genes related to extracellular matrix remodeling, angiogenesis, fibroblast activation and tumor progression (**Figure 4A**) and these genes are well-established mediators of cancer-associated fibroblast (CAF) in lung cancer **[19]**. TIMP1, MMP1 and MMP9 are central regulators of matrix turnover and invasive remodeling, while FLT1 (VEGFR1), ESM1 and PLVAP are associated with angiogenic signaling and vascular-stromal communication **[20, 21]**. TNFAIP6, ADAMTS family members and COL10A1 further suggest active tissue remodeling and wound-healing-like stromal activation **[22, 23]**. Integrin-related genes such as ITGA1 and ITGAV, together with extracellular matrix components including LAMB1, COMP and PXDN, indicate enhanced adhesive and structural interactions between stromal cells, vasculature and tumor cells **[24, 25]**. Conversely, stromal cells distal to tumor cells demonstrated relative downregulation of genes associated with vascular quiescence, homeostatic stromal function, metabolic regulation, or less activated mesenchymal states **[26]**. This suggests that stromal

ISSN 0973-2063 (online) 0973-8894 (print)
Bioinformation 22(7): 3954-3962 (2026)

cells near tumor cells undergo substantial phenotypic reprogramming away from tissue-maintaining functions toward a specialized reactive state. Similarly, module scoring of the tumor-proximal stromal gene signature further confirmed the reproducibility across studies (**Figure 4B**). Gene Set Enrichment Analysis of tumor-proximal stromal upregulated genes showed enrichment in ECM organization, wound healing, cell adhesion, fibroblast proliferation and tissue morphogenesis (**Figure 4C**). Enriched pathways also included blood vessel development, angiogenesis, vasculature development and coagulation. Immune-related pathways enriched included adaptive immune response, B cell-mediated immunity, lymphocyte-mediated immunity, complement activation, humoral immune response and B cell receptor signaling. These findings suggest that tumor-proximal stromal cells may play underappreciated roles in immune niche organization, potentially influencing tertiary lymphoid structure formation and immune cell recruitment within the NSCLC microenvironment. Spatial Immune Reprogramming in Tumor-Proximal Immune Cells Beyond stromal and endothelial compartments, SPADE further revealed that multiple immune populations undergo spatially structured transcriptional reprogramming in response to proximity to malignant cells (**Figure S1-S3 A**). In the myeloid compartment, tumor-proximal cells showed increased expression of CD74 and C1QC, together with MRC1, suggesting enhanced antigen presentation capacity coupled with tumor-associated macrophage-like immunoregulatory features **[27]**. Within the B/plasma cell compartment, upregulation of TNFAIP3, CXCL9 and TMEM173 indicated activation of inflammatory signaling and innate immune sensing programs **[28, 29]**. Similarly, tumor-proximal T/NK cells exhibited elevated IL21 and CXCL9 expression, consistent with enhanced cytokine-mediated immune activation and chemotactic signaling within the tumor-adjacent niche **[30]**. Validation in the independent NSCLC cohort confirmed reproducibility of the tumor-proximal immune signatures across cell types **(Figure S1-S3 B)**. Tumor-proximal B/plasma and T/NK programs showed significant enrichment in the external dataset, consistent with the discovery cohort while the myeloid signature showed a trend toward significance ($p = 0.083$). Overall, these results indicate that SPADE identified reproducible spatial transcriptional signatures across multiple cell types.

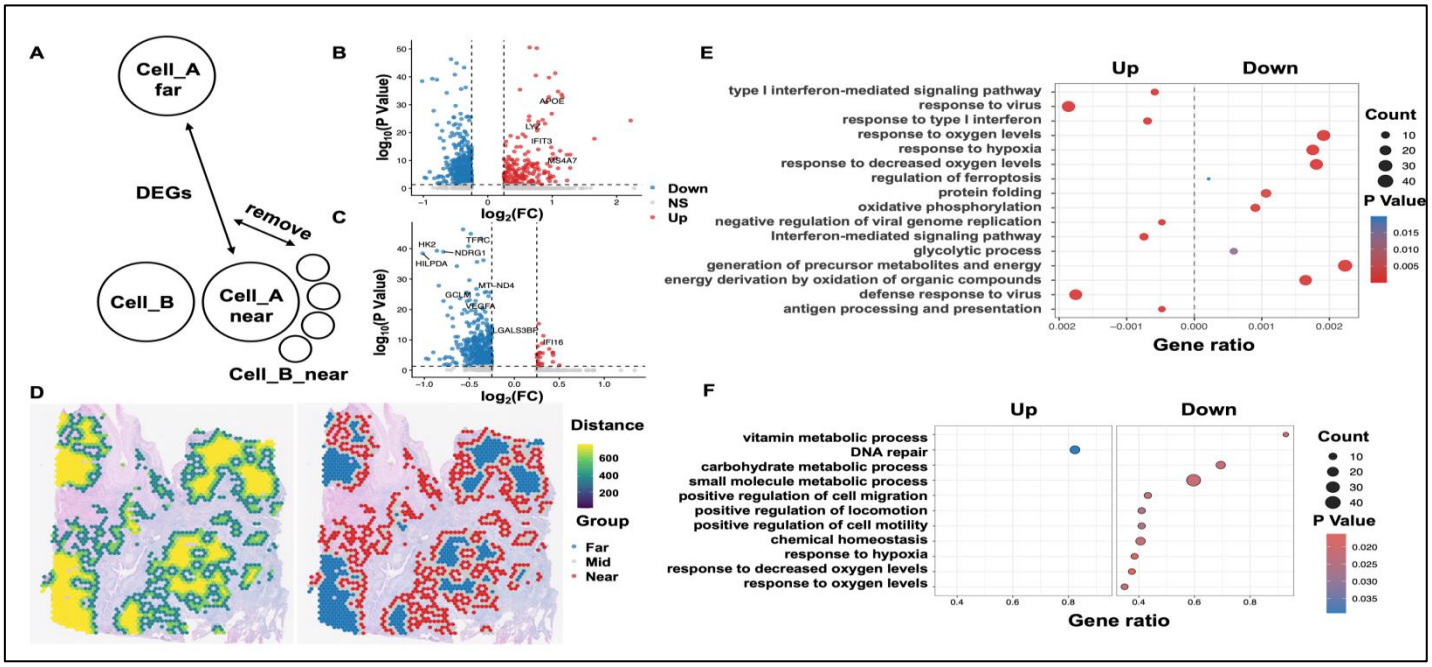

Figure 1: SPADE enables contamination-aware identification of spatially resolved differential expression. (A) Schematic overview of the SPADE workflow. For each cell type of interest, SPADE calculates the spatial distance from each cell to its nearest neighboring cell of a reference cell type, then compares gene expression between cells falling within a defined "near" distance threshold versus those beyond a "far" distance threshold, while controlling for confounding expression changes using a separate control analysis. (B) Volcano plot showing differentially expressed genes identified by conventional differential expression analysis without contamination control. (C) Volcano plot showing differentially expressed genes identified by SPADE between epi-like lung tumor cells located proximal versus distal to myeloid cells. (D) Schematic illustration of spatial distance-based grouping. Epi-like tumor cells are classified as "near", "mid", or "far" based on their distance to the nearest myeloid cell. (E) Gene Ontology (GO) enrichment analysis of genes upregulated in tumor-proximal epi-like cells compared to tumor-distal cells. (F) Gene Set Enrichment Analysis (GSEA) revealing activation of type I interferon signaling and antiviral response pathways in tumor cells located in close proximity to myeloid cells.

ISSN 0973-2063 (online) 0973-8894 (print)
Bioinformation 22(7): 3954-3962 (2026)

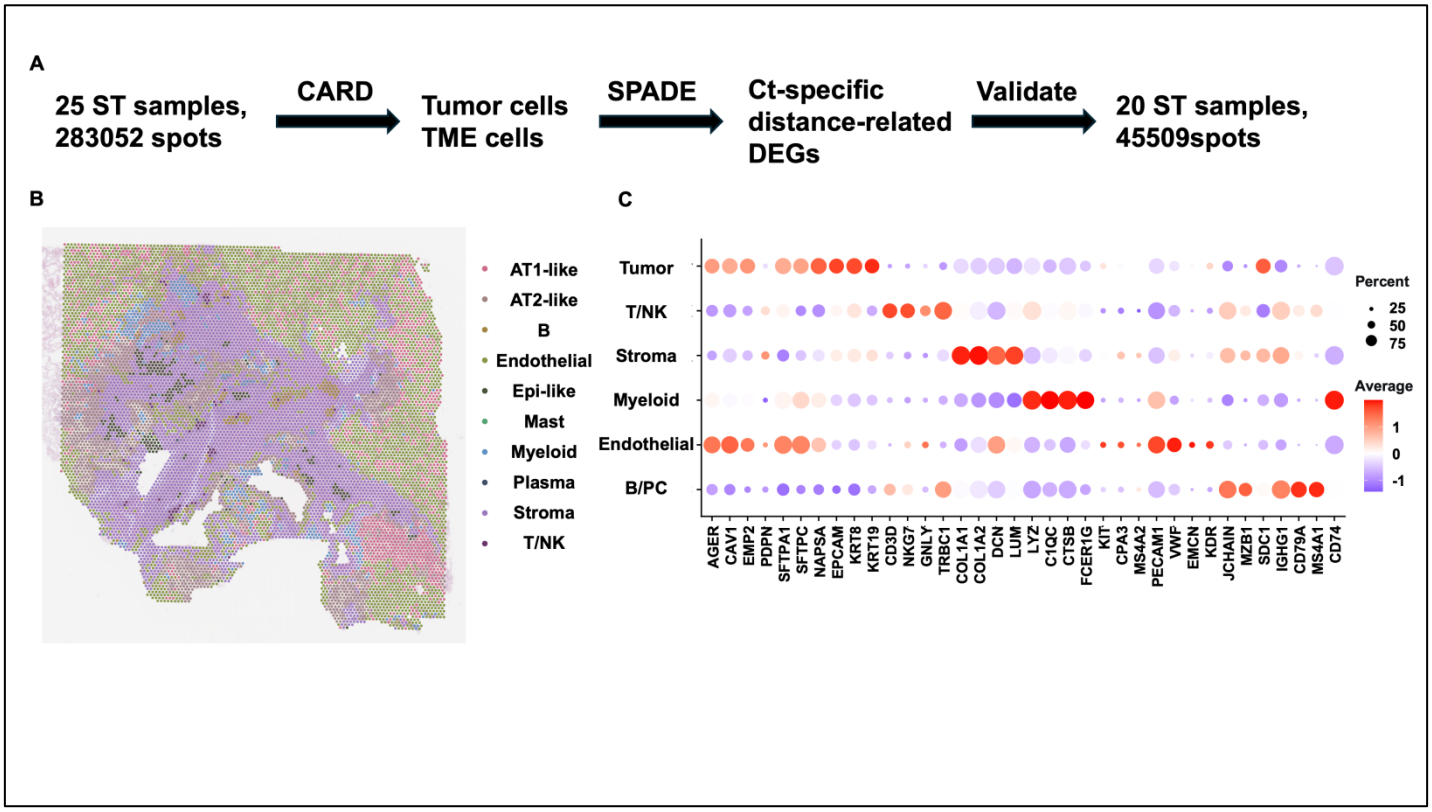

Figure 2: Systematic application of SPADE to discovery and validation cohorts of NSCLC spatial transcriptomics samples. (A) Study design flowchart. SPADE was applied to a discovery cohort of 25 non-small cell lung cancer (NSCLC) spatial transcriptomics samples comprising 283,052 spots, with cell types annotated using CARD. Differentially expressed genes between tumor-proximal and tumor-distal cells were identified within each sample using SPADE. The resulting spatially associated gene signatures were then validated in an independent cohort of 20 additional NSCLC spatial transcriptomics samples. (B) Spatial distribution of annotated cell types in a representative NSCLC sample from the discovery cohort. (C) Dot plot showing expression levels of canonical marker genes across annotated cell types. Dot size represents the percentage of cells expressing each marker and color intensity represents average expression level.

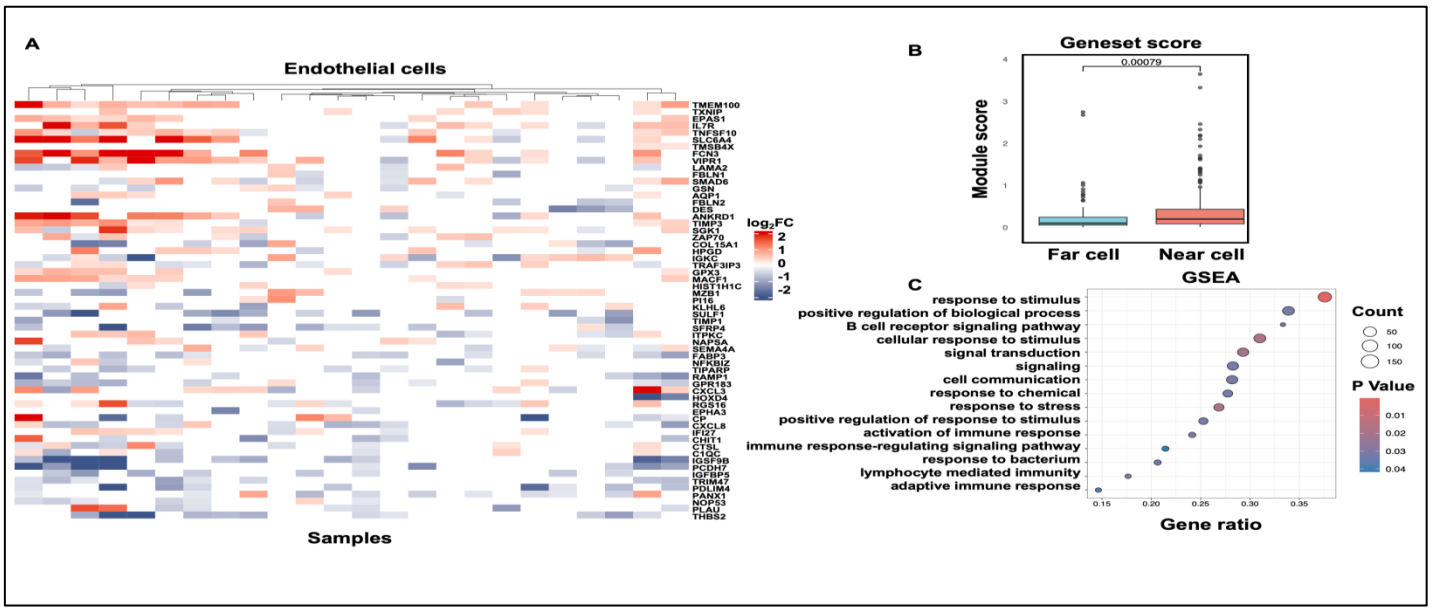

ISSN 0973-2063 (online) 0973-8894 (print)

Bioinformation 22(7): 3954-3962 (2026)

Figure 3: Tumor-proximal endothelial cells exhibit vascular homeostasis and immune-responsive programs in NSCLC. (A) Heatmap showing SPADE-identified differentially expressed genes in endothelial cells across samples. Endothelial cells were compared between those located proximal versus distal to tumor cells. Rows represent genes consistently significant in at least three independent samples, columns represent individual samples. Color scale indicates $\log_2$ fold. (B) Module scoring of the tumor-proximal endothelial upregulated gene signature in an independent NSCLC spatial transcriptomics validation cohort. (C) Gene Set Enrichment Analysis (GSEA) of genes upregulated in tumor-proximal endothelial cells performed on the independent validation cohort.

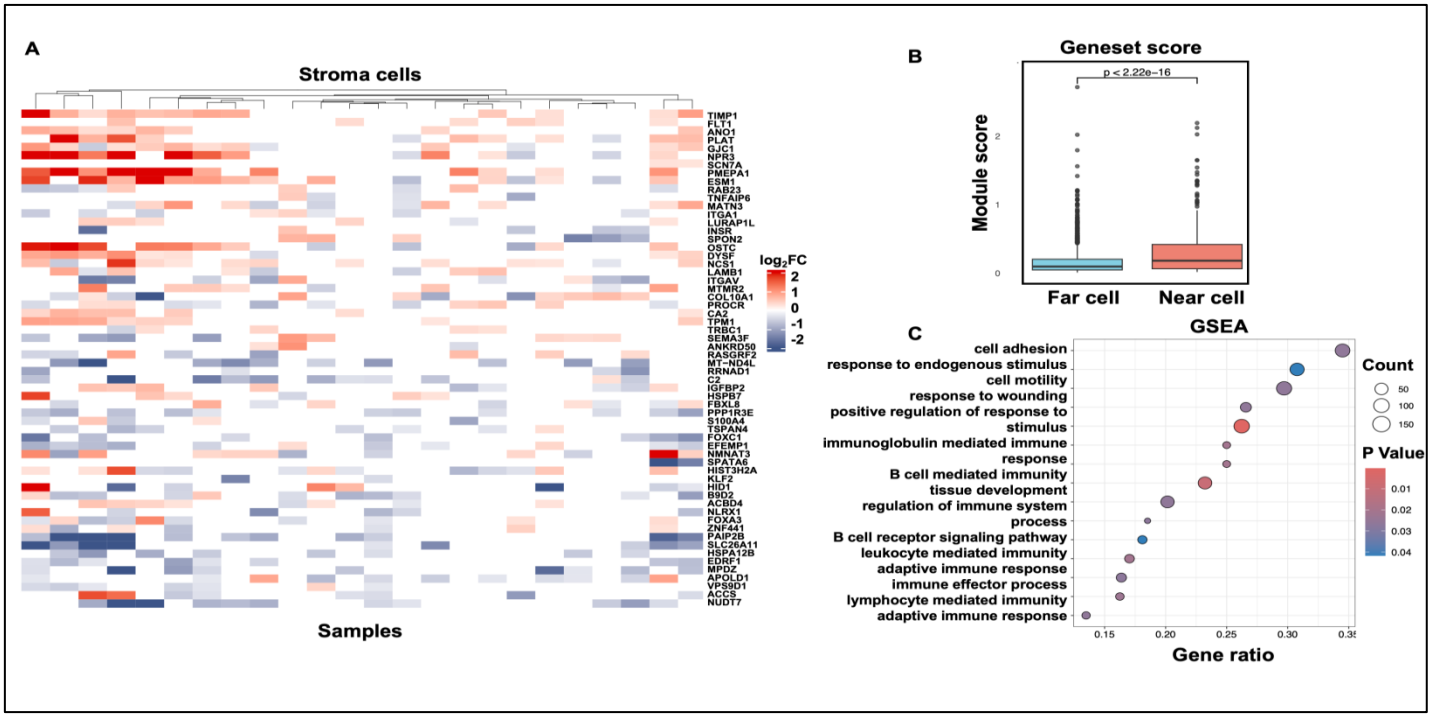

Figure 4: Tumor-proximal stromal cells display activated ECM remodeling and immunomodulatory programs. (A) Heatmap showing SPADE-identified differentially expressed genes in stroma cells across samples. Stroma cells were compared between those located proximal versus distal to tumor cells. Rows represent genes consistently significant in at least three independent samples, columns represent individual samples. Color scale indicates $\log_2$ fold. (B) Module scoring of the tumor-proximal stroma upregulated gene signature in an independent NSCLC spatial transcriptomics validation cohort. (C) Gene Set Enrichment Analysis (GSEA) of genes upregulated in tumor-proximal stroma cells performed on the independent validation cohort.

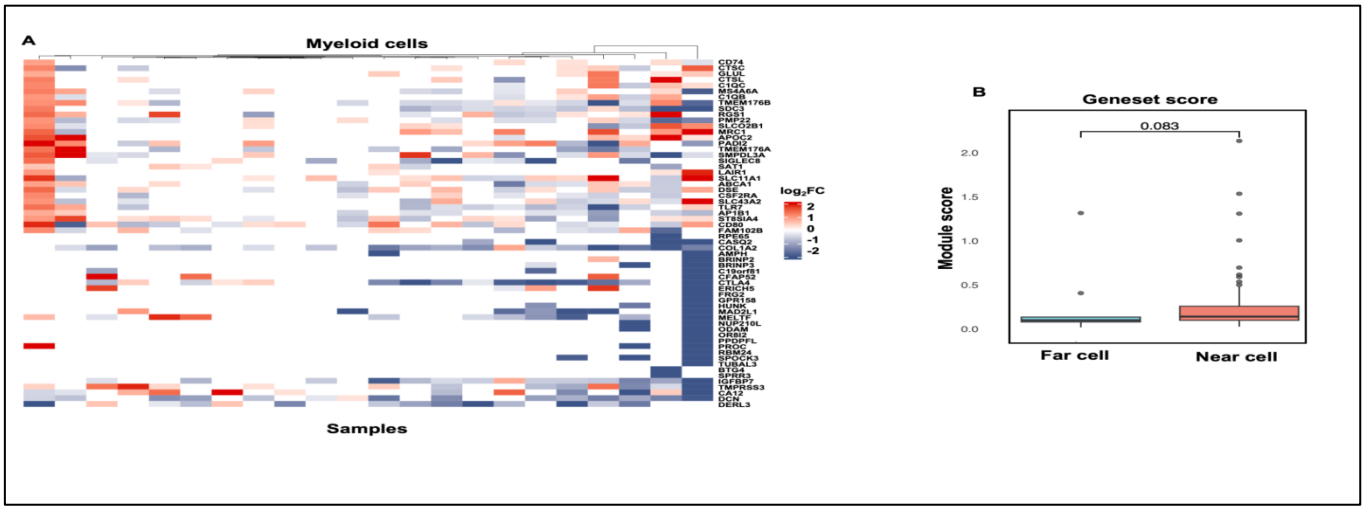

ISSN 0973-2063 (online) 0973-8894 (print)
Bioinformation 22(7): 3954-3962 (2026)

Figure S1: Tumor-proximal myeloid cells exhibit enhanced antigen presentation and immunoregulatory features. (A) Heatmap showing SPADE-identified differentially expressed genes in myeloid cells across samples. Myeloid cells were compared between those located proximal versus distal to tumor cells. Rows represent genes consistently significant in at least three independent samples, columns represent individual samples. Color scale indicates log2 fold. (B) Module scoring of the tumor-proximal myeloid upregulated gene signature in an independent NSCLC spatial transcriptomic validation cohort.

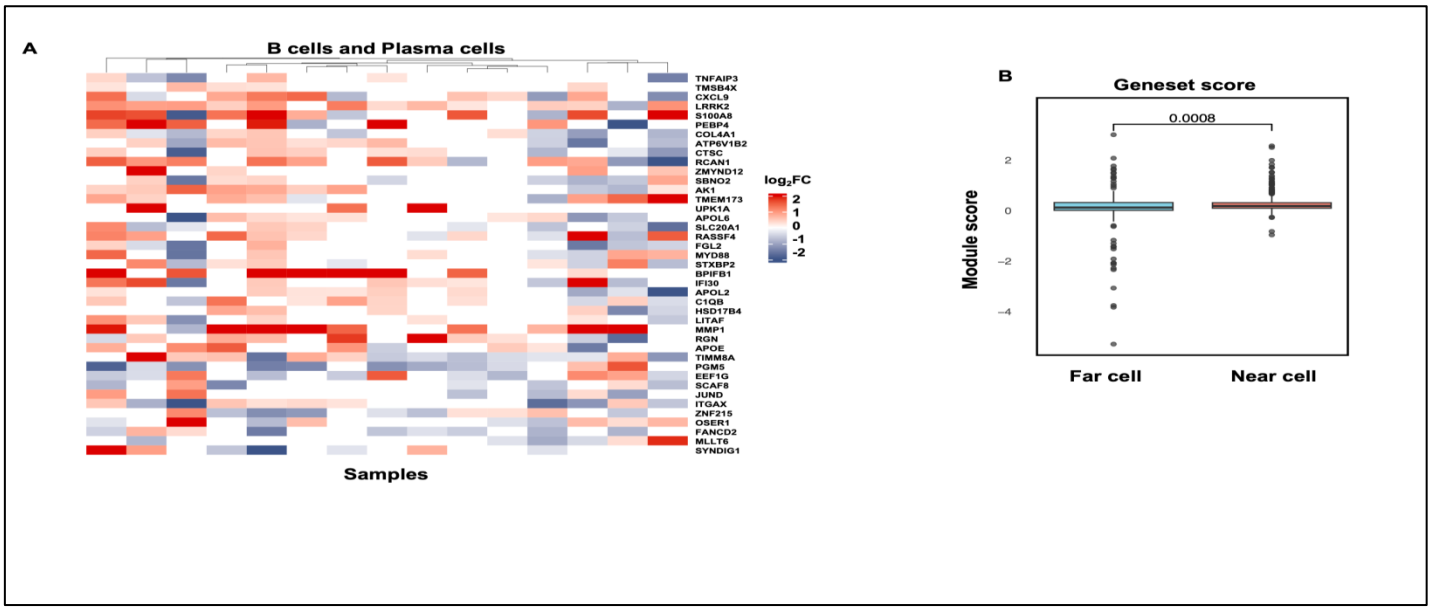

Figure S2: Tumor-proximal B/plasma cells activate inflammatory signaling and innate immune sensing programs. (A) Heatmap showing SPADE-identified differentially expressed genes in B/plasma cells across samples. B/plasma cells were compared between those located proximal versus distal to tumor cells. Rows represent genes consistently significant in at least three independent samples, columns represent individual samples. Color scale indicates log_2 fold. (B) Module scoring of the tumor-proximal B/plasma upregulated gene signature in an independent NSCLC spatial transcriptomics validation cohort.

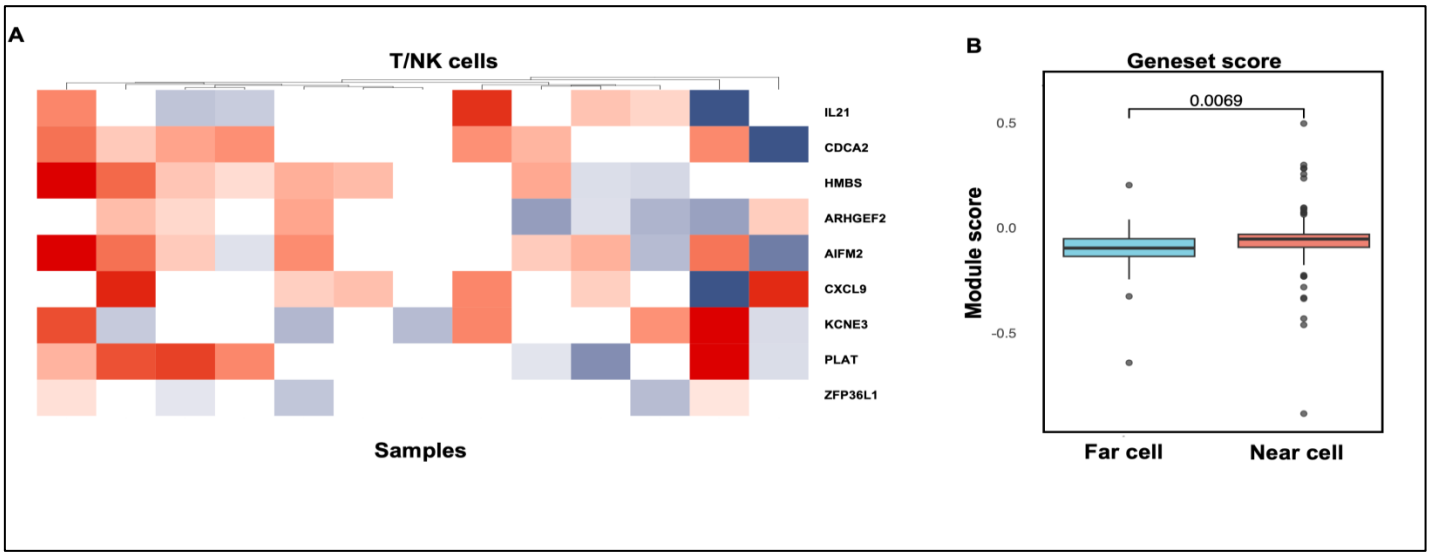

Figure S3: Tumor-proximal T/NK cells exhibit enhanced cytokine-mediated activation and chemotactic signaling. (A) Heatmap showing SPADE-identified differentially expressed genes in T/NK cells across samples. T/NK cells were compared between those located proximal versus distal to tumor cells. Rows represent genes consistently significant in at least three independent samples, columns represent individual samples. Color scale indicates log_2 fold. (B) Module scoring of the tumor-proximal T/NK upregulated gene signature in an independent NSCLC spatial transcriptomic validation cohort.

Discussion:

In this study, we introduced SPADE, an R package designed to quantify the distance-dependent gene expression changes while controlling for contamination from adjacent cells. This is particularly important when each spot in ST can contain mixed signals from multiple cell types and deconvolution-based annotation is often required **[31]**. By integrating seamlessly with Seurat objects, SPADE enables researchers to compare cells located near versus far from a cell type of interest, with a built-in control analysis to filter out confounding expression signals. To systematically evaluate SPADE's performance, we applied it to a large cohort of 25 NSCLC spatial transcriptomics samples comprising over 280,000 spots, with cell types annotated using CARD. By identifying differentially expressed genes between tumor-proximal and tumor-distal TME cells within each sample and then validating the resulting gene sets in an independent cohort of 20 additional ST samples, we established a rigorous pipeline for discovering reproducible spatial transcriptional signatures. Our analysis of endothelial cells revealed a striking spatial dichotomy. Tumor-proximal endothelial cells upregulated genes associated with pulmonary capillary identity and vascular homeostasis, while distal endothelial cells expressed markers of inflammatory signaling and endothelial-to-mesenchymal transition. These observations are consistent with prior studies showing that tumor-associated endothelial cells are not merely structural vascular components but can actively regulate immune-cell trafficking and vascular remodeling **[32, 33].** Tumor-proximal stromal fibroblasts exhibited a pronounced activated phenotype with a strong enrichment of extracellular matrix organization, wound healing, and angiogenesis pathways. These results are in line with the well-established roles of cancer-associated fibroblasts in extracellular matrix remodeling, tissue repair-like activation, angiogenesis, invasion, and therapeutic resistance **[34]**. Notably, the simultaneous enrichment of complement activation, B cell-mediated immunity, and humoral immune response pathways suggests a role for tumor-proximal stromal cells in orchestrating local immune niches **[35]**. Beyond endothelial and stromal compartments, SPADE revealed that diverse immune populations undergo spatially structured transcriptional reprogramming in response to tumor proximity. While the myeloid signature showed only a trend toward significance in the validation cohort, the consistent directional effect across cell types and cohorts suggests that SPADE can nominate candidate distance-related transcriptional signatures that merit further validation. This is particularly relevant because myeloid cells in NSCLC are known to be highly heterogeneous and spatially variable, and higher-resolution spatial or single-cell validation may be required to distinguish macrophage, monocyte, and dendritic-cell-specific programs **[36]**. Several limitations of this study should be acknowledged. First, while SPADE effectively filters out contamination from adjacent cells by leveraging control analyses, the resolution of spatial transcriptomics remains limited by spot size and sequencing depth. Future integration with higher-resolution platforms or combined single-cell and spatial approaches could further refine proximity assignments. Second, our analyses are correlational as SPADE identifies genes whose expression differs by distance but does not establish causal relationships between spatial proximity and transcriptional change. Third, our validation cohort, while independent, was similarly derived from NSCLC samples; whether these spatial programs generalize to other cancer types or to non-malignant disease contexts remains an open question.

Conclusion:

SPADE provides a contamination-aware and distance-based framework for identifying spatially organized transcriptional programs in complex tissues. Applied to NSCLC spatial transcriptomic datasets, SPADE revealed reproducible proximity-associated changes in endothelial, stromal, and immune compartments, highlighting its potential as a practical tool for studying tumor–microenvironment interactions and generating spatially informed biological hypotheses.

Author contribution:

Mingke Wu: Conceptualization, Software, Formal analysis, Writing – original draft, Writing – review & editing, Visualization.

Acknowledgements:

Not applicable.

Competing interests:

The authors declare no competing interests.

References:

[1] Hunter MV *et al. Nat Commun.* 2021 **12**:6278 [PMID: 34725363]
[2] Jin Y *et al. Mol Cancer.* 2024 **23**:129 [PMID: 38902727]
[3] Long KA *et al. The Plant Cell.* 2026 **38**:koaf282 [PMID: 41388990]
[4] Wang Q *et al. Small Methods.* 2025 **9**:2401107 [PMID: 39760243]
[5] Moses L & Pachter L. *Nat Methods.* 2022 **19**:534 [PMID: 35273392]
[6] Larsson L *et al. Nat Methods.* 2021 **18**:15 [PMID: 33408402]
[7] Ma Y & Zhou X. *Nat Biotechnol.* 2022 **40**:1349 [PMID: 35501392]
[8] Hao Y *et al. Nat Biotechnol.* 2024 **42**:293 [PMID: 37231261]
[9] Gaspard-Boulinc LC *et al. Nat Rev Genet.* 2025 **26**:828 [PMID: 40369312]
[10] Yan L & Sun X. *Bioinformatics.* 2023 **39**:btac805 [PMID: 36515467]
[11] Bergenstråhle L *et al. Nat Biotechnol.* 2022 **40**:476 [PMID: 34845373]
[12] De Zuani M *et al. Nat Commun.* 2024 **15**:4388 [PMID: 38782901]
[13] Gillich A *et al. Nature.* 2020 **586**:785 [PMID: 33057196]
[14] Wang N *et al. Front. Cell Dev. Biol.* 2023 **11**:1125723 [PMID: 36923253]
[15] Liu B *et al. ATVB.* 2022 **42**:1495 [PMID: 36252125]
[16] He M *et al. BMC Pulm Med.* 2023 **23**:116 [PMID: 37055764]

[17] Schupp JC *et al. American Journal of Respiratory and Critical Care Medicine.* 2023 **208**:819 [PMID: 37552025]
[18] Zeng Q *et al. Nat Rev Cancer.* 2023 **23**:544 [PMID: 37349410]
[19] Sahai E *et al. Nat Rev Cancer.* 2020 **20**:174 [PMID: 31980749]
[20] Xie L *et al. Clin Transl Med.* 2025 **15**:e70532 [PMID: 41431249]
[21] Craig-Schapiro R *et al. Nat Commun.* 2025 **16**:1338 [PMID: 39915484]
[22] Chou C-H *et al. Sci Rep.* 2020 **10**:10868 [PMID: 32616761]
[23] Sebastian A *et al. Int J Mol Sci.* 2020 **21**:364 [PMID: 31935848]
[24] Goveia J *et al. Cancer Cell.* 2020 **37**:21 [PMID: 31935371]
[25] Moreira HR *et al. npj Regen Med.* 2022 **7**:57 [PMID: 36167724]
[26] Lee C *et al. Sig Transduct Target Ther.* 2025 **10**:170 [PMID: 40383803]
[27] Liu C *et al. Front Immunol.* 2025 **16**:1690992 [PMID: 41394809]
[28] Gopalakrishnan RP *et al. Nat Commun.* 2026 **17**:3200 [PMID: 41741475]
[29] Cabeza-Cabrerizo M *et al. Annu. Rev. Immunol.* 2021 **39**:131 [PMID: 33481643]
[30] Chen S *et al. Clin Exp Med.* 2024 **24**:204 [PMID: 39196390]
[31] Elosua-Bayes M *et al. Nucleic Acids Research.* 2021 **49**:e50 [PMID: 33544846]
[32] Alnaqbi H *et al. Trends in Cancer.* 2024 **10**:1072 [PMID: 39289084]
[33] Carman CV & Martinelli R. *Front. Immunol.* 2015 **6**:603 [PMID: 26635815]
[34] Siddhartha R & Garg M. *Molecular Cancer Therapeutics.* 2023 **22**:291 [PMID: 36861362]
[35] Thiery J. *Explor Target Antitumor Ther.* 2022 **3**:598 [PMID: 36338519]
[36] Liu X *et al. Translational Oncology.* 2024 **50**:102143 [PMID: 39366301]